Spring 5-19-2009

Towards Improved Accuracy of Gravitational Waves Extraction

Maria Babiuc-Hamilton
Marshall University, babiuc@marshall.edu

Recommended Citation
Babiuc, M. C. (2008, August) Towards Improved Accuracy of Gravitational Wave Extraction. Slides presented at 2008 Numerical Relativity and Data Analysis Meeting, Syracuse, NY.

Towards Improved Accuracy of the Gravitational Waves Extraction

Maria C. Babiuc

Department of Physics, Marshall University

Huntington, WV

2008 Numerical Relativity and Data Analysis Meeting

Syracuse, NY, Aug.11 2008

Abstract

- Results in developing two new methods to improve the accuracy of waveform extraction using characteristic evolution.
- Numerical method: circular boundaries, with angular dissipation in the characteristic code.
- Geometric method: computation of Weyl tensor component Ψ_4 at null infinity, in a conformally compactified treatment.
- Comparison and calibration in tests problems based upon linearized waves.

Introduction

- The artificial finite outer boundary present in Cauchy codes introduce two sources of error:
- The outer boundary condition,
- Waveform extraction at an inner worldtube.
- The problem of proper boundary condition for a radiating system can be solved only by extension to I^4 (conformal compactification).
- Cauchy Characteristic Extraction (CCE) offers a means to avoid these errors.

Introduction

- The CCE code extends the solution to $\mathcal{I}^+$ by matching the interior Cauchy evolution to an exterior characteristic evolution.
- The code uses the data on a worldtube provided by binary black hole spacetimes obtained with any Cauchy evolution codes, and computes the gravitational radiation reaching infinity in terms of the supplied boundary data.

Sources of Error

- Perturbative regime tests compares favorably CCE with Zerilli extraction, and show CCE advantage at small radii.
- Nonlinear tests show CCE stable, but plagued by numerical error in the numerical postprocesing at null infinity.
- Two ways: numeric and geometric, to improve the accuracy of the waveform.

Ways to improve accuracy

- Geometrical: computation of the asymptotic of part of Ψ_4 and comparison with the news *N*.
- Numerical: improvement of intergrid interpolations between the patches smoothly covering the sphere. Comparison between:
- The circular stereographic patching,
- The cubed-sphere patching.
- Alternatives: higher order finite difference approximations, adaptive mesh refinement.

Characteristic Formulation

- Based on a family of outgoing null hypersurfaces, from the worldtube to infinity, in Bondi-Sachs metric:

$$ds^2 = -\left(e^{2\beta}\frac{V}{r} - r^2 h_{AB}U^A U^B\right)du^2 - 2e^{2\beta}dudr - 2r^2 h_{AB}U^B dudx^A + r^2 h_{AB}dx^A dx^B$$

$$J = \frac{1}{2}h_{AB}q^A q^B, \quad q_{AB} = \frac{1}{2}\left(q_A \bar{q}_B + \bar{q}_A q_B\right)$$

- The Einstein equations $\boldsymbol{G_{\mu\nu}=0}$ decompose into hypersurface, evolution and conservation equations. The evolution equation takes the form:

$$2(rJ)_{,ur} - \left(r^{-1}V(rJ)_{,r}\right)_{,r} = -r^{-1}\left(r^2\eth U\right)_r + 2r^{-1}e^{\beta}\eth^2 e^{\beta} - \left(r^{-1}V\right)_{,r}J + N_J$$

- The code implements this as a second order finite difference scheme, all angular derivatives first order.

Angular dissipation

- Numerical dissipation is necessary to:
  - stabilize the intergrid interpolation error,
  - suppress the circular boundary high frequency error
- The evolution equation takes the form:

$$\partial_u\left((1-x)\Phi_{,x}+\Phi\right)=S, \quad x=r/(R+r), \quad \Phi=xJ,$$

- We introduce angular dissipation in the retarded time *u* and radial *r* evolutions:

$$\partial_u\left((1-x)\Phi_{,x}+\Phi\right)\to\partial_u\left((1-x)\Phi_{,x}+\Phi\right)+\varepsilon_u h^3\eth^2 W\bar{\eth}^2\partial_u\left((1-x)\Phi_{,x}+\Phi\right)$$

$$\partial_u\left((1-x)\Phi_{,x}+\Phi\right)\to\partial_u\left((1-x)\Phi_{,x}+\Phi\right)+\varepsilon_x h^3\eth^2 W\bar{\eth}^2\Phi_{,u}$$

- We dissipate also the hypersurface equations.

Waveforms at null infinity

- Conformal Penrose compactification of Bondi metric:

$$l = 1/r, \quad \hat{g}_{\mu\nu} = l^2 g_{\mu\nu}$$

$$\hat{g}_{\mu\nu} dx^\mu dx^\nu = -\left(e^{2\beta} V l^3 - h_{AB} U^A U^B\right) du^2 + 2e^{2\beta} du dl - 2h_{AB} U^B du dx^A + h_{AB} dx^A dx^B$$

- Future null infinity ***I*⁺** is at *l=0*. The Bondi mass (total energy), news *N* and Ψ_4^0 (radiation power), are constructing from expansion of metric in powers of *l*.

$$2H_{C(A} D_{B)} L^C + \partial_u H_{AB} - H_{AB} D_C L^C = O(l)$$

- H, H_{AB}, c_{AB} and L^A are expansion coefficients.
- One can require the Bondi coordinate to be inertial (Minkowsky) at ***I*⁺** but it is not assumed: the waveform characteristic extraction is done in null coordinates.

Calculation of the News

- In an inertial conformal Bondi frame the News are :

$$N = \lim_{\Omega \to 0} \frac{1}{2\Omega} Q^{\alpha} Q^{\beta} \tilde{\nabla}_{\alpha} \tilde{\nabla}_{\beta} \Omega$$

- where:

$$\tilde{g}_{\mu\nu} = \Omega^2 g_{\mu\nu} = \omega^2 \hat{g}_{\mu\nu}, \quad \Omega = \omega l, \quad Q_{AB} := \tilde{g}_{ab}\big|_{I^+} = \omega^2 H_{AB}$$

$$H^{AB} = \left(F^A \overline{F}^B + \overline{F}^A F^B\right)/2 \; F^A = q^A \sqrt{\frac{K+1}{2}} - \overline{q}^A J \sqrt{\frac{1}{2(K+1)}}, Q^{\beta} = e^{-i\delta} \omega^{-1} F^{\beta} + \lambda \tilde{n}^{\beta}$$

- An explicit calculation leads to:

$$N = \frac{1}{4} e^{-2i\delta} \omega^{-2} e^{-2H} F^{\alpha} F^{\beta} \left\{ \left(\partial_u + \pounds_L\right) c_{AB} - \frac{1}{2} c_{AB} D_C L^C + 2\omega D_A \left[\omega^{-1} D_B \left(\omega e^{2H}\right)\right] \right\}$$

- In inertial Bondi coordinates: $N = \frac{1}{4} Q^A Q^B \partial_u c_{AB}$
- The general form is used, which is challenging because of second order angular derivatives of ω.

Calculation of Weyl tensor

- Weyl tensor vanishes at ***I*⁺** (asymptotic flatness)

$$\hat{\Psi} := -\frac{1}{2}\lim_{l\to 0}\frac{1}{l}\hat{n}^{\mu}\hat{m}^{\nu}\hat{n}^{\rho}\hat{m}^{\sigma}\hat{C}_{\mu\nu\rho\sigma} = -\frac{1}{2}\overline{\Psi_4}^{0}, \quad \hat{n}^{\mu} = \hat{\nabla}^{\mu} l, \quad \hat{l}^{\mu}\partial_{\mu} = \partial_{l}$$

- The inertial radiation field in terms of code variables:

$$\Psi = \frac{1}{2}\omega^{-3}e^{-2i\delta}\hat{n}^{\mu}F^{A}F^{B}\left(\partial_{\mu}\hat{\Sigma}_{AB} - \partial_{A}\hat{\Sigma}_{\mu B} - \hat{\Gamma}^{\alpha}_{\mu B}\hat{\Sigma}_{A\alpha} + \hat{\Gamma}^{\alpha}_{AB}\hat{\Sigma}_{\mu\alpha}\right)\Big|_{I^{+}}$$

- involves lengthy algebra. In inertial Bondi coordinates

$$\Psi = \frac{1}{4}Q^{A}Q^{B}\partial_{\mu}^{2}c_{AB} = \partial_{\mu}^{2}\partial_{l}J\Big|_{I^{+}} = \partial_{u}N.$$

- However, general form is used, which is challenging because of third order angular derivatives of ω.

Linearized Expressions

- The general nonlinear representation of Ψ in terms of the computational variables reduces to a simpler form in first order perturbations off Minkowski background.

$$\Psi = \frac{1}{2}\partial_u^2\partial_l J - \frac{1}{2}\partial_u J - \frac{1}{2}\eth L - \frac{1}{8}\eth^2\left(\eth L + \bar{\eth} L\right) + \partial_u \eth^2 H$$

$$N = \frac{1}{2}\partial_u\partial_l J + \frac{1}{2}\eth^2\left(\omega + 2H\right)$$

- This provide a starting point to compare the advantages between computing the radiation via the Weyl component or the news function.
- ω propagates across patches $2\hat{n}^\alpha\partial_\alpha \log\omega = -e^{-2H} D_A L^A$.

Patching the Sphere

- The nonsingular description of smooth tensor fields on the sphere requires more than one coordinate patch.
- We consider two treatments: the stereographic, using 2 patches, and the cubed-sphere, using 6 patches.
- In the stereographic approach, every point on the sphere is covered by at least one of the patches, and around equator, points are covered by two patches.
- We implement the circular stereographic method, based on the **composite-mesh method**, where the overlap is reduced to a circular region around equator.

Circular patches

- Complex stereographic coordinates cover the sphere

$$\xi_N = q_N + ip_N = \tan(\theta/2)e^{i\varphi}, \xi_S = 1/\xi_N$$

$$F_S(\xi_S = 1/\xi_N) = F_N(\xi_N)(-1)^s e^{-2is\varphi}$$

- Unit sphere metric in each patch:

$$q_{AB}dx^A dx^B = \frac{4}{P^2}(dq^2 + dp^2), P = 1 + q^2 + p^2, q^A = \frac{P}{2}(1,i), \sqrt{q^2 + p^2} = 1$$

- All boundary points of one patch are interior points of another patch. The overlapping of the patches is key to the stability of method. The discretization is:

$$q_i = -1 + (i - O - 1)\Delta, p_j = -1 + (j - O - 1)\Delta, 1 \le i, j \le M + 1 + 2O$$

- The active finite difference grid: $\sqrt{q_i^2 + p_j^2} \le 1 + (O - R_E)\Delta$
- Stability requires that the interpolation stencil for one patch ghosts points lies below equator in other patch.

The cubed sphere

- Sphere covered by 6 coordinate patches, obtained by by projecting 6 faces of a circumscribed cube.
- Recently applied to characteristic evolution **gr-qc/0610019**
- For M^2 stereographic grid points, there are $\pi M^2/4$ grid cells inside equator on each hemisphere.
- In the cubed sphere grid, with N^2 points per patch, the entire sphere is covered by $6 x N^2$ points. This gives:

$$N^2 \approx (\pi/12) M^2$$

- The tests are run with $M=100,120$ for the circular patch, which correspond to $N=51,61$ for cubed-sphere, $t=120$.
- We monitor the convergence and smoothness of error:

$$\varepsilon(\Phi) = \left\| \Phi_{numeric} - \Phi_{analytic} \right\|_\infty$$

Comparison between circular and cubed methods

- A test of 2D wave propagation on the sphere:

$$-\partial_t^2\Phi + \eth\bar{\eth}\Phi = 0, \Phi = \cos(\omega t)Y_{lm}, \omega = \sqrt{l(l+1)}$$

- Allows direct comparison between the circular patches and the cubed-sphere methods, without characteristic evolution and Ψ_4 and ***N*** computation.
- Angular dissipation, necessary for the circular case:

$$\partial_t^2\Phi \to \partial_t^2\Phi + \varepsilon\Delta^3 D^4 \partial_t\Phi, D^4\Phi = \left(P^2/4\left(D_{+q}D_{-q} + D_{+p}D_{+p}\right)\right)^2\Phi$$

- Emphasis on the accuracy of the angular derivatives required by Ψ_4 and ***N*** in the waveform extraction.

Error in Φ and $\delta^2\Phi$

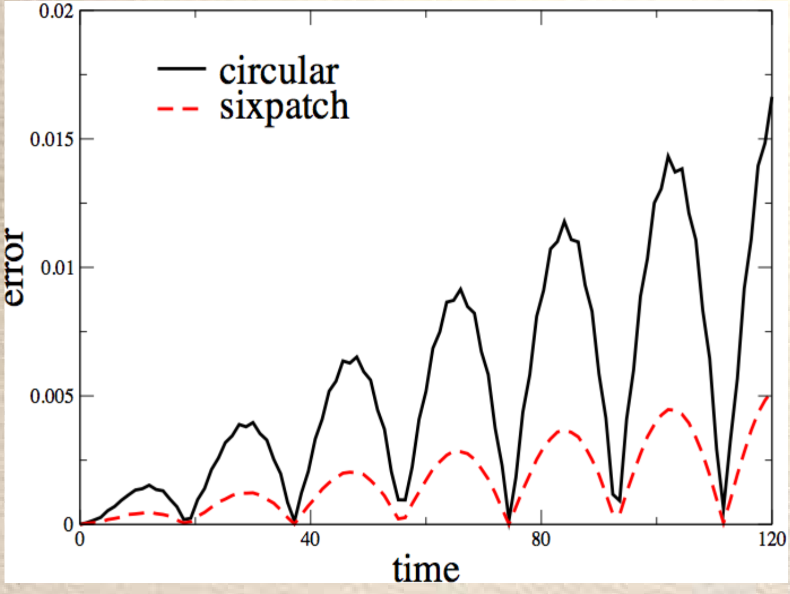

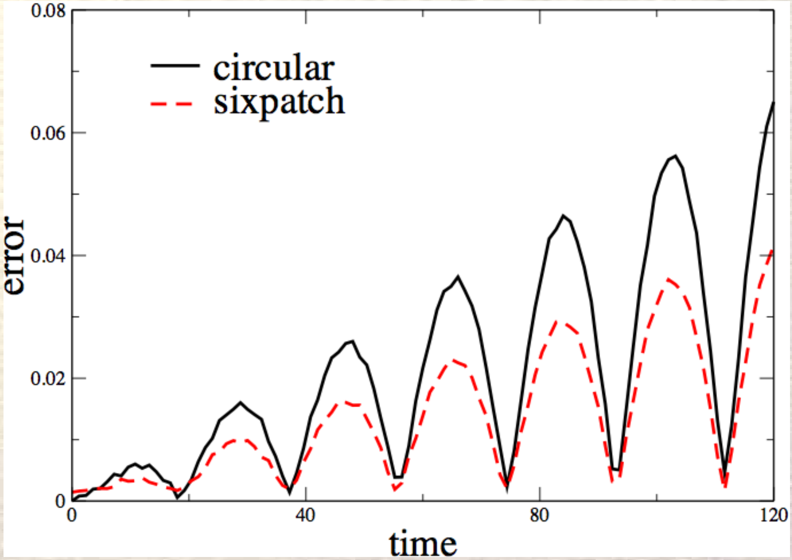

Algrthm	T=1.2	T=12	T=102	T=120
circular	2.00	1.99	1.99	2.00
cubed	1.99	1.97	1.98	1.99

Algrthm	T=1.2	T=12	T=102	T=120
circular	2.02	1.95	1.99	2.01
cubed	1.95	2.02	2.00	1.97

Error in $\delta^3 \Phi$

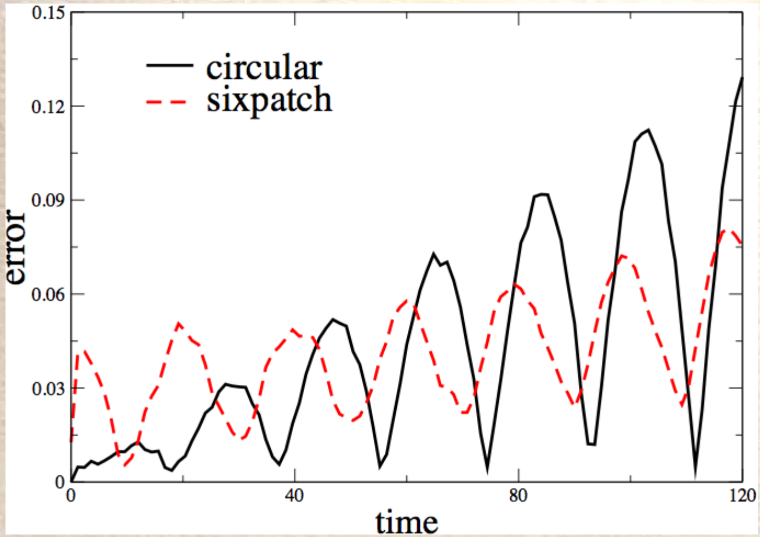

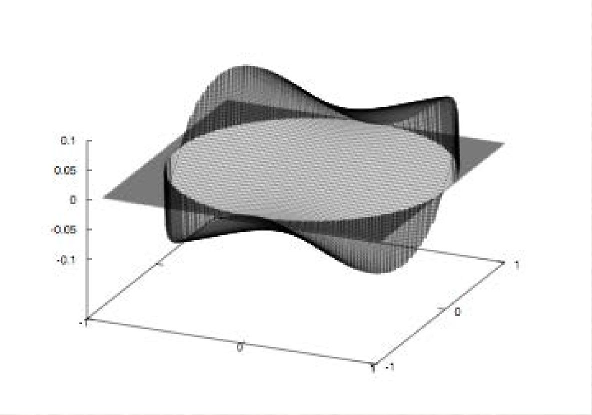

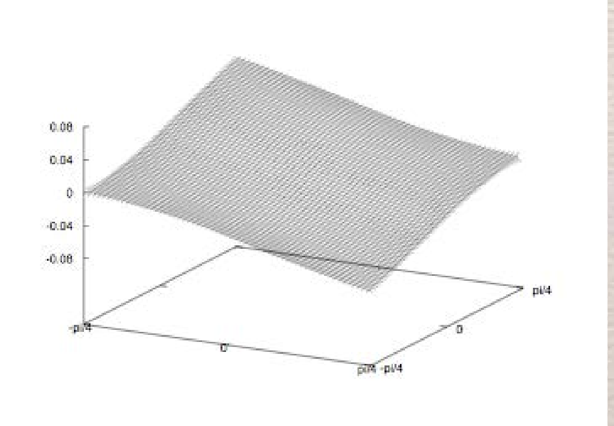

Algrthm	T=1.2	T=12	T=102	T=120
circular	2.28	2.03	1.99	2.01
cubed	1.11	0.88	2.01	1.96

Our choice

- For $\varepsilon(\Phi)$, clear 2nd order convergence for both methods is observed. The cubed sphere error is smaller than the stereographic error (1/3).
- For $\varepsilon(\delta^2\Phi)$, the cubed sphere error is 2/3 the stereographic error. Again, 2nd order convergence.
- For $\varepsilon(\delta^3\Phi)$ the cubed sphere method shows poor convergence at early times.
- Until t=60, the cubed-sphere method has the largest error, but at the end, is 4/5 the stereographic error.
- These results justify our choice of the circular patches stereographic method in the comparison of the news *N* and Weyl tensor Ψ_4 extraction.

Comparisons of News and Weyl tensor extraction

- We base the test on a class of solutions in Bondi-Sachs form to the linearized vacuum Einstein equation on a Minkowski background:

$$J = \sqrt{(l-1)l(l+1)(l+2)}\,{}_2Y_{lm}\,\mathrm{Re}(J_l(r)e^{i\nu u})$$

$$N = \mathrm{Re}\left(e^{i\nu u}\lim_{r\to\infty}\left(-\frac{l(l+1)}{4}J_l - \frac{i\nu}{2}r^2 J_{r,l}\right) + e^{i\nu u}\beta_l\right)\sqrt{(l-1)l(l+1)(l+2)}\,{}_2Y_{lm}$$

$$\Psi = N_{,u}, \quad N_\Psi = N\big|_{u=0} + \int_0^u \Psi du$$

- Solution: well-behaved at **I⁺** and well-defined at $r>r_0>0$

$$J_2(r) = \frac{24\beta_0 + 3i\nu C_1 - i\nu^3 C_2}{36} + \frac{C_1}{4r} - \frac{C_2}{12r^3}, \; J_3(r) = \frac{60\beta_0 + 3i\nu C_1 + \nu^4 C_2}{180} + \frac{C_1}{10r} - \frac{i\nu C_2}{6r^3} - \frac{C_2}{4r^4}$$

$$C_1 = 3\cdot 10^{-6}, C_2 = 10^{-6}, \beta_0 = i\cdot 10^{-6}$$

Test results for *J*

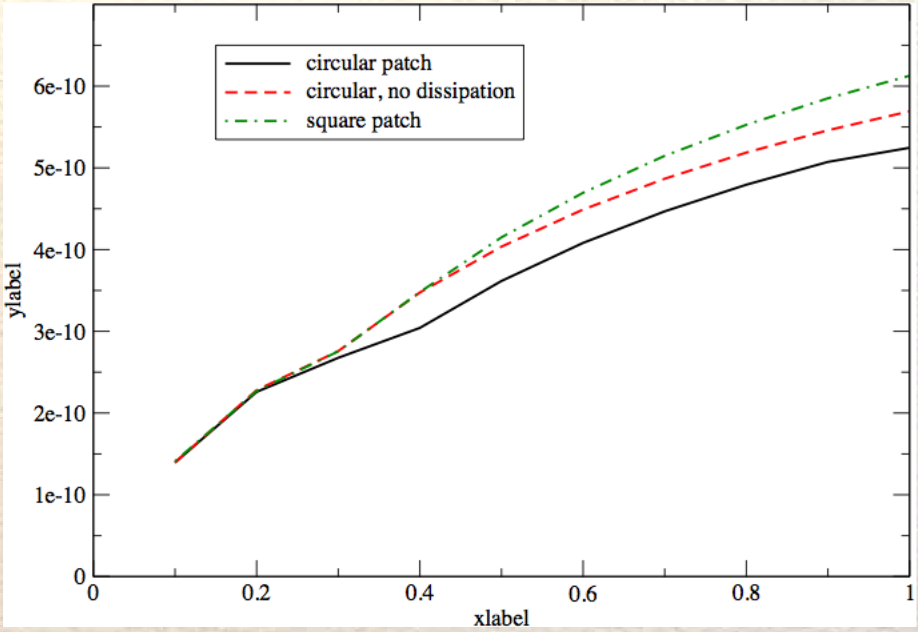

- Runs with circular patch, circular without dissipation, and the original square patch methods. The plots show that error increases with x and is maximum at I+. Also, that angular dissipation reduces the error.

Convergence for *J*

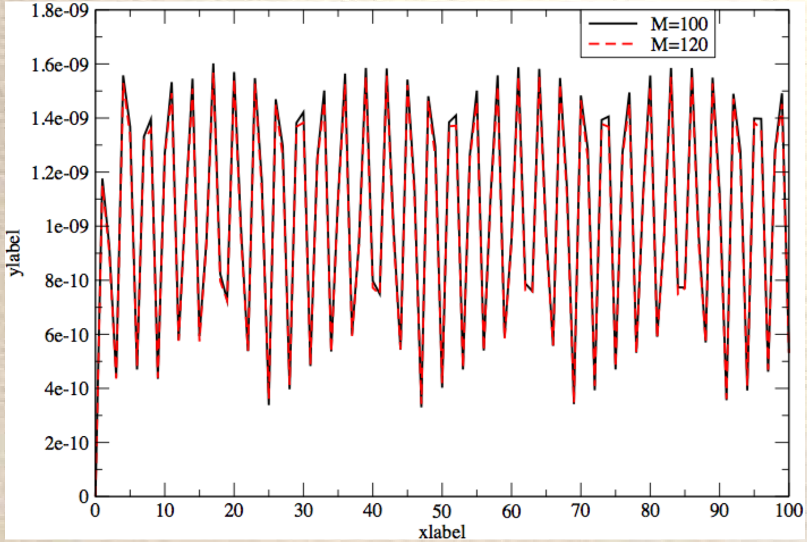

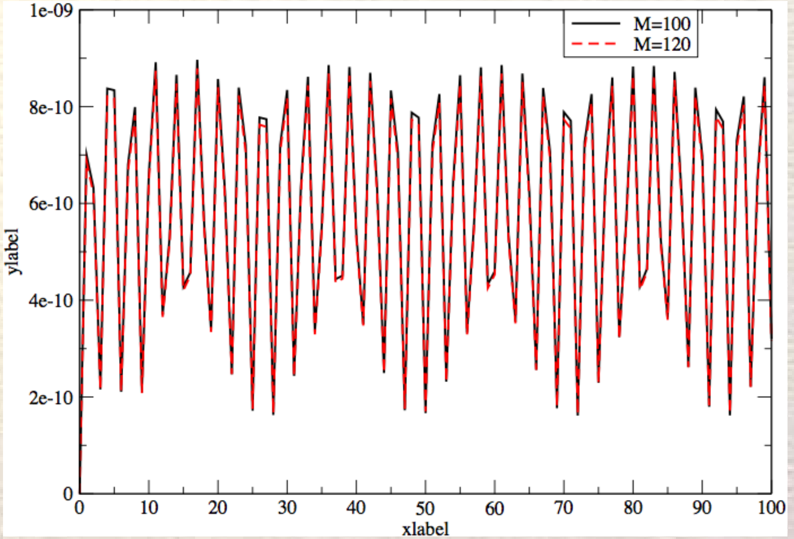

Vrbl	circle	crnods	square
T=1	2.01	2.01	2.01
T=10	1.95	2.00	1.99
T=90	2.07	1.96	2.00
T=100	1.92	2.01	1.99

Vrbl	circle	crnods	square
T=1	2.02	2.02	2.02
T=10	1.99	1.99	2.00
T=90	2.02	2.02	2.04
T=100	2.00	2.00	1.99

Surface Plots for *J*

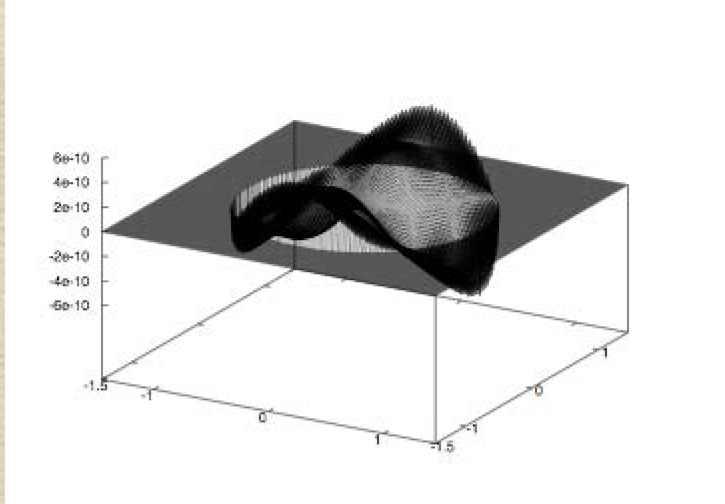

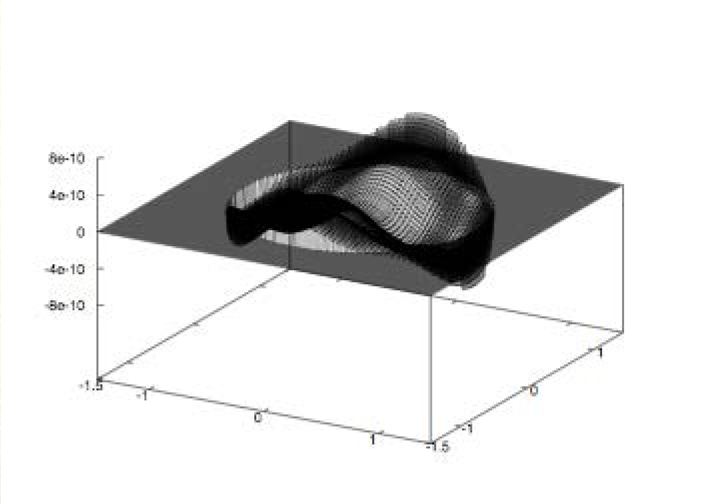

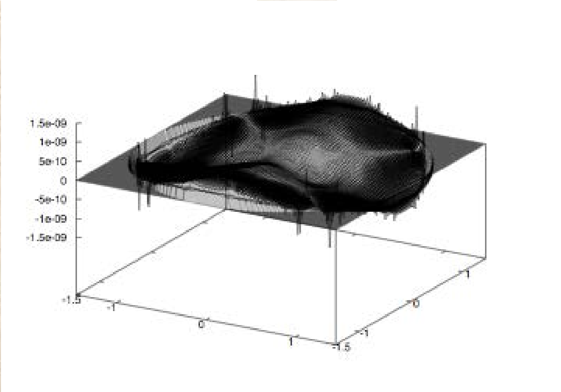

Test results for the news: N *(left)* and N_Ψ *(right)*

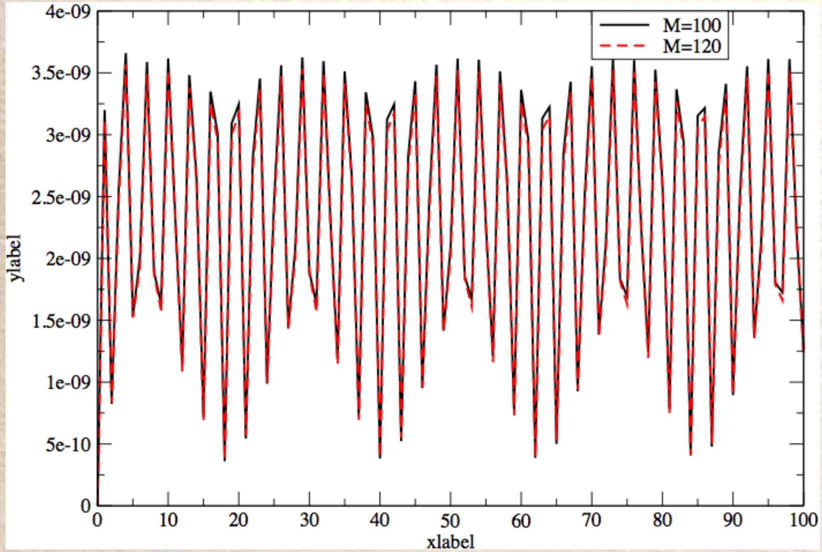

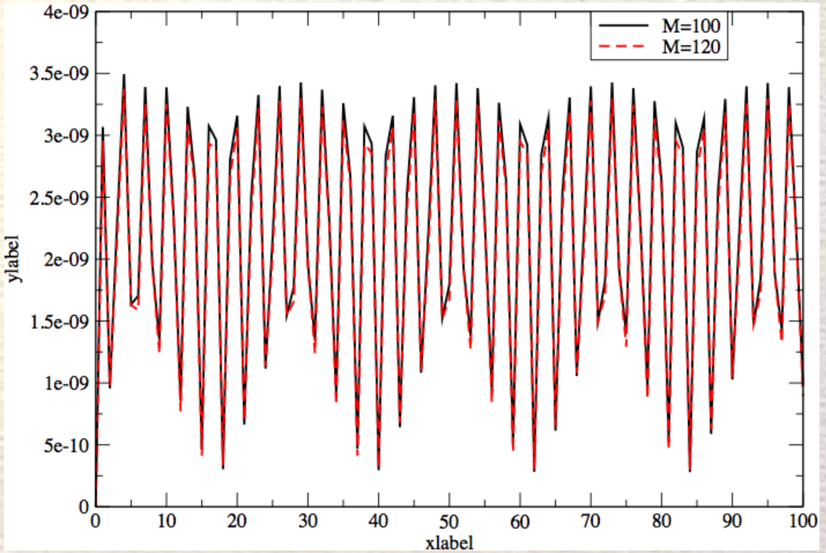

Vrbl	circle	crnods	square
T=1	2.04	2.04	2.04
T=10	2.04	1.99	2.04
T=90	2.01	2.01	2.06
T=100	1.98	2.00	1.93

Vrbl	circle	crnods	square
T=1	2.08	2.08	2.08
T=10	2.09	2.05	2.10
T=90	2.05	2.00	2.06
T=100	1.98	2.01	1.93

Surface Plots for N

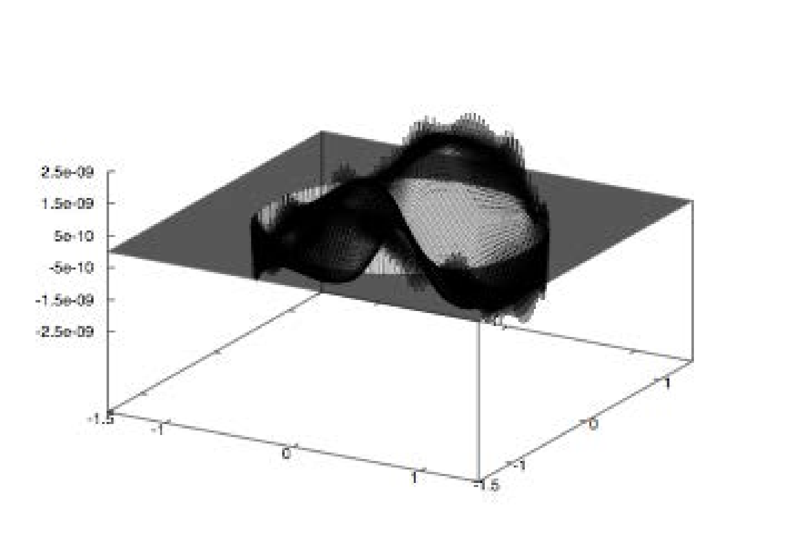

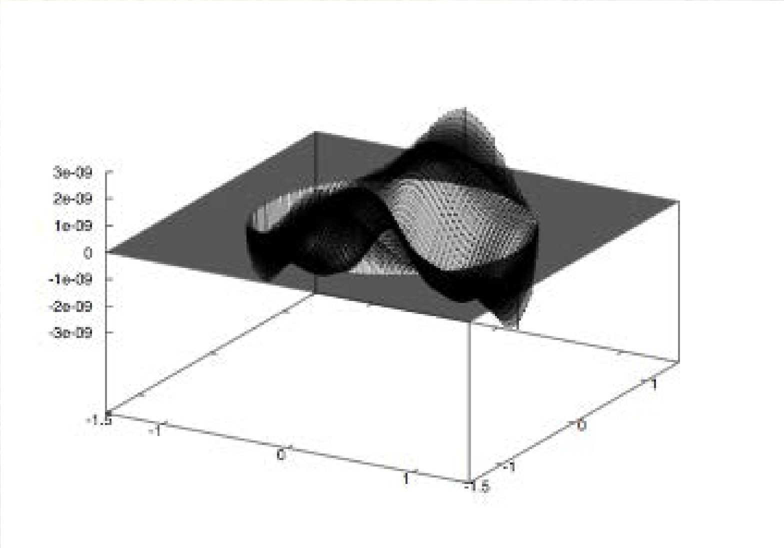

- Effectiveness in applying dissipation. Slightly more jaggedness near the equator for the circular patches is overbalanced by the relative smallness of its error.

Surface Plots for N_{Ψ}

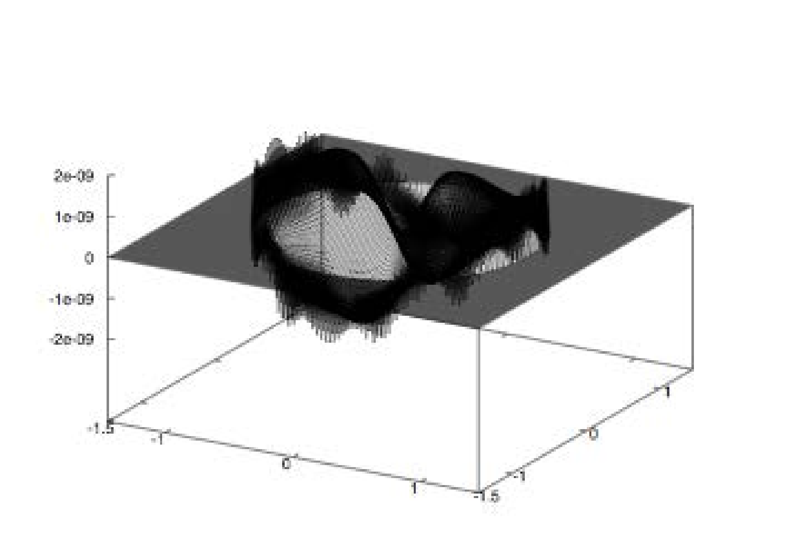

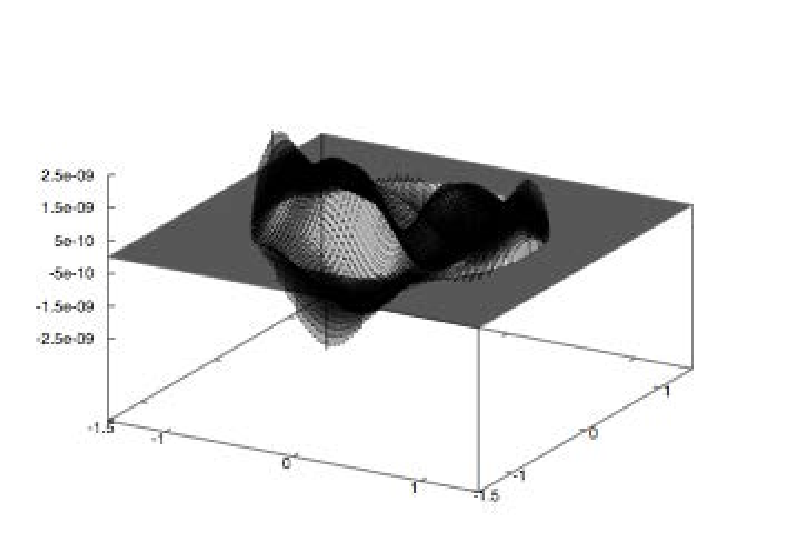

- The error in N_{Ψ} is slightly smaller, otherwise there is little difference between N and N_{Ψ}.

Vrbl	circle	crnods	square
N	2.25×10^{-9}	3.32×10^{-9}	2.90×10^{-9}
N_{Ψ}	1.71×10^{-9}	2.75×10^{-9}	2.32×10^{-9}

Conclusions

- For linearized case no method is clear winner.
- The news calculated on a circular patch had lower error than that on a square patch (30%).
- Weyl tensor extraction is slightly more accurate than news function extraction (24%).
- Very small fractional error (0.1%) in metric J.
- The corresponding averaged error in the N_{Ψ} and N was 4% for the circular patch runs and the maximum error at the equator was 9%.

Conclusions

- All errors were second order convergent.
- The errors did not vary appreciably (30%) with the choice of discretization method.
- Intrinsic difficulty in extracting waveforms due to the delicate cancellation of leading order terms in the metric and connections.
- The excellent accuracy that we find for the metric suggests that perturbative waveform extraction must suffer the same difficulty.

Conclusions

- Waveforms are not easy to extract accurately.
- The convergence of the error is a positive sign that higher order finite difference approximations might supply the accuracy needed for realistic astrophysical applications.
- Whether the advantages the new methods proposed here prove to be significant will depend upon the results of future application in the nonlinear regime.

Thanks

- Collaboration: Nigel Bishop, Bela Szilagyi, Jeff Winicour
- **Strategies for the Characteristic Extraction of Gravitational Waveforms (*arXiv:0808.0861)***
- M. C. Babiuc, N. T. Bishop, B. Szilagyi, J. Winicour, submitted to Physical Review D
- Open Source CCM: we work toward making the characteristic extraction module available to the numerical relativity community.